

Supporting Information

Multifunctional and robust composite materials comprising gold nanoparticles at a spherical polystyrene particle surface

Samir A. Belhout,^a Ji Yoon Kim,^a David T. Hinds,^a Natalie Owen,^b Jonathan A. Coulter^b and Susan J. Quinn^{a*}

E-mail: susan.quinn@ucd.ie

^aSchool of Chemistry, University College Dublin, Belfield, Dublin 4, Ireland

^bSchool of Pharmacy, Queen's University Belfast, BT9 7BL, UK

Experimental

Materials

Chloroauric acid, sodium citrate, hydrochloric acid, sodium chloride (NaCl), ethanol (EtOH), phosphate buffered saline tablets (PBS) and sodium borohydride were all supplied from Sigma Aldrich. Nitric acid was supplied by Riedel-de Haen. Amine-modified polystyrene beads were supplied by Life technology. Dulbecco's Modified Eagle Medium (DMEM) and Foetal Bovine Serum (FBS) were supplied by Gibco BRL. All materials were analytical grade and were used without any further purification. All water was obtained from an ultra-pure Millipore 0.22 µm filtration system (18.2 mΩ conductivity)

Characterisation

UV-visible (UV-vis) spectroscopy (Varian Cary-50 Eclipse spectrophotometer) was used to characterize the synthesised AuNPs as well as the composite materials. Atomic absorption spectroscopy (AAS) (Varian SpectrAA 55B atomic absorption spectrometer) was used to determine the quantity of AuNPs on the surface of the composite materials. Dynamic light scattering (DLS) and zeta potential measurements were carried out on a Malvern Zetasizer Nano-ZS. Agitation was performed using a Grant-bio PCMT Thermo shaker. Centrifugation was carried out using a Thermo Scientific Heraeus pico 17 centrifuge. All transmission electron microscopy (TEM) images were captured using a Jeol 2100 at 100 kV accelerating voltage in the Centre for Microscopy and Analysis in Trinity College, Dublin. Scanning electron microscopy (SEM) images were capture in the Advanced Microscopy Laboratory in Trinity College Dublin.

4.5 nm AuNPs synthesis¹

Sub 5-nm AuNPs were synthesised via a preparation modified from a paper by Jana, Gearhart and Murphy. Briefly, chloroauric acid (0.0098 g) and sodium citrate (0.0074 g) were dissolved in 20 mL of ddH₂O in a 100 mL conical flask. This was set to stir vigorously at room temperature. 1 mL of 0.125 M ice cold sodium borohydride was then injected into the vortex of the mixture. The formation of nanoparticles was indicated by the appearance of an orange-red colour instantly. The as synthesised nanoparticles were characterized by UV-vis, AAS and TEM.

15nm & 26 nm AuNPs synthesis²

A range of sizes of gold nanoparticles were prepared via the seeded growth method developed by Puentes. Briefly, a seed solution was prepared by injecting 1 mL of chloroauric acid solution (25 mM) into 150 mL of a boiling solution of sodium citrate (2.2 mM) contained in a 3 neck round bottom flask and fitted with a reflux condenser and thermometer. The reaction was allowed to proceed for 15 min and then cooled to 90 °C.

1 mL of chloroauric acid solution (25 mM) was injected into the seed solution and allowed react for 30 min. This was repeated twice. After the third addition had reacted for 30 min, 55 mL of sample was harvested and replaced with 53 mL of ddH₂O and 2 mL of sodium citrate solution (60 mM). This acted as the seed solution for the next generation. This process was repeated four times. The as synthesized gold nanoparticles were characterized using UV-visible spectroscopy, atomic absorption spectroscopy, dynamic light scattering and transmission electron microscopy.

General procedure for composite preparation

Various concentrations of gold nanoparticles were added to a range of samples containing constant concentrations of polystyrene spheres. The samples were then agitated at 1000 rpm for 60 min at 25 °C. The samples were then centrifuged (1500 – 5000 rpm, 15 min), depending on the gold nanoparticle size, in order to pellet any composite material and leave free gold nanoparticles in the supernatant. The pellet was analysed by UV-visible spectroscopy, atomic absorption spectroscopy, dynamic light scattering and transmission electron microscopy. The supernatant was analysed by UV-visible spectroscopy and atomic absorption spectroscopy. Fully occupied composites were put through a centrifugation redispersion cycle, with the retention of optical absorbance monitored by UV-Vis of the redispersed pellet and leeching of AuNPs from the surface of the PS monitored by AAS of the supernatant

Ionic strength and physiological buffer stability study

Fully occupied composite particles (4.5 nm AuNPs@, 15 nm AuNPs@ and 26 nm AuNPs@200 nm PS) were formed following the same procedure as above. All unbound free gold was removed through centrifugation washing. The washed composite materials were then centrifuged down and redispersed separately in 1 mL of ddH₂O, 70 % EtOH, 250 mM NaCl, 350 mM NaCl, 500 mM NaCl, 10 mM PBS and DMEM supplemented with FBS (10 %). The UV-Vis absorbance was taken of each at time 0 and then at 24 h intervals for 72 h. The retention of optical properties was evaluated by normalizing each absorbance value vs. the absorbance value for H₂O at time 0.

Alamar Blue Assay

1 x 10⁴ cells were plated in a 96 well plate (Nunc, UK) with 100 µl of complete media and incubated for 24 h allowing adhesion. Cells were treated with 4.5 nm AuNP@200 nm PS composite particles at a concentration of 10 or 25 µg/mL for 24 h at 37°C in 5% CO₂ / 95% air. Nanoparticle doped medium was then removed and cells washed in PBS. 10% Alamar blue (Invitrogen) was added to complete growth medium and incubated at 37°C in 5% CO₂ / 95% air for 4 h. 50 µl of the Alamar blue containing medium was added to a 96 well blackout flat bottom plate and the fluorescence measured at 585 nm using a FLUOstar optima plate reader (BMG labtech, GE). The percentage of surviving cells was calculated relative to untreated controls.

Hyperspectral methodology

Enhanced darkfield optical images were captured using a Cytoviva microscope. Using improved alignment and oblique angle illumination, the darkfield condenser enhances the signal-to-noise of nanoscale samples, enabling optical visualisation of nanoparticle scattered light. Following treatment (described above) cells were fixed in 10% formalin for 15 min, and mounted in Vectashield with DAPI, a non-specific DNA stain (excitation 358 nm emission 461 nm).

General procedure for catalytic reduction of 4-nitrophenol to 4-aminophenol

Sodium borohydride (2.5 mL, 10 mM) was added to a quartz cuvette (3 mL, 1 cm) along with 4-nitrophenol (12.5 µL, 10 mM). To this a stir bar was added and the solution de-gassed for 10 min using a flow of nitrogen. 100 µL of the composite solution was injected into the cuvette, with the concentration normalized for surface area of polystyrene added. The UV-visible spectra were acquired over the range 200-600 nm at 25 °C at 15 s intervals.

Determination of % PS coverage, PS Surface area occupied per AuNP, % Au Weight and AuNP Surface Area per weight

Average Maximum Loading (max. load_{avg})

$$\text{max. load}_{\text{avg}} = \frac{\text{max.load}_{UV-Vis} + \text{max.load}_{AAS} + \text{max.load}_{CompAAS}}{3}$$

% Polystyrene Surface Area Coverage (% PS SA Coverage)

$$\text{Surface Area Polystyrene Bead (SA}_{PS}) = 4\pi(r_{PS})^2$$

$$\text{Exclusion Area of 1 AuNP (EA}_{AuNP}) = \pi(r_{AuNP})^2$$

$$\text{Total Exclusion Area (EA}_{TOT}) = EA_{AuNP} \times \text{max. load}_{\text{avg}}$$

$$\% \text{ PS SA Coverage} = \frac{EA_{TOT}}{SA_{PS}} \times 100$$

PS Surface Area occupied per AuNP assuming uniform distribution (SA_{PS} per AuNP)

$$\text{SA}_{PS} \text{ per AuNP} = \frac{SA_{PS}}{\text{max.load}_{\text{avg}}}$$

% AuNP Weight per Weight of Composite Particle (% Au Weight)

$$\text{Total AuNP Weight (Wgt}_{AuNPs}) = \left(\frac{4}{3}\pi(r_{AuNP})^3 \times \rho_{Au}\right) \times \text{max. load}_{\text{avg}}$$

$$\text{PS Weight (Wgt}_{PS}) = \left(\frac{4}{3}\pi(r_{PS})^3 \times \rho_{PS}\right)$$

$$\% \text{ Au Weight} = \frac{Wgt_{AuNPs}}{Wgt_{AuNPs} + Wgt_{PS}} \times 100$$

AuNP Surface Area per Weight of Composite Particle (AuNP SA per Weight)

$$\text{Total AuNP Surface Area (AuNP SA}_{TOT}) = 4\pi(r_{AuNP})^2 \times \text{max. load}_{\text{avg}}$$

$$\text{AuNP SA per Weight} = \frac{AuNP SA_{TOT}}{Wgt_{AuNPs} + Wgt_{PS}}$$

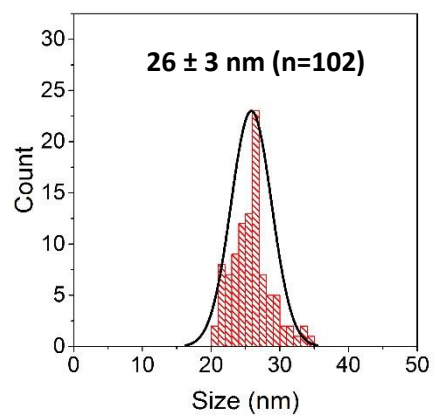
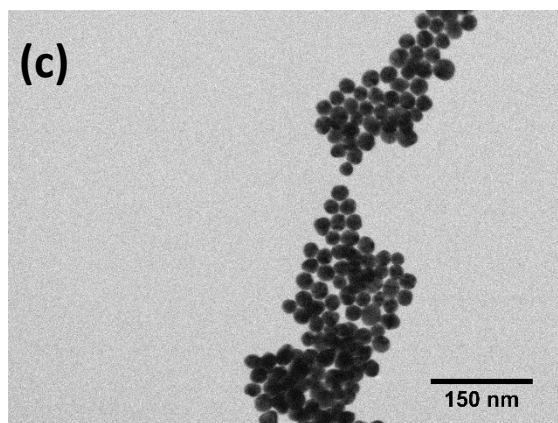
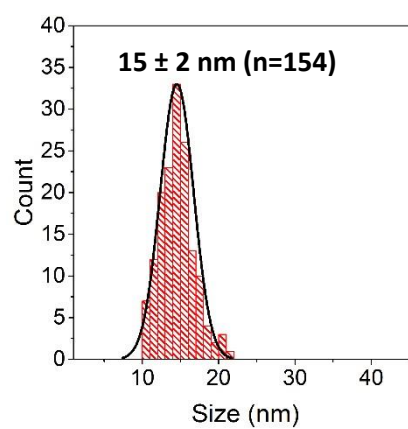
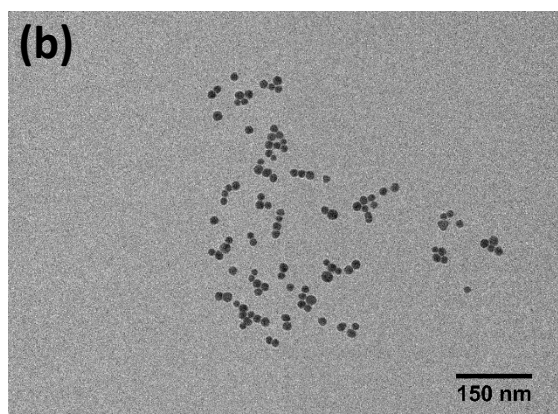
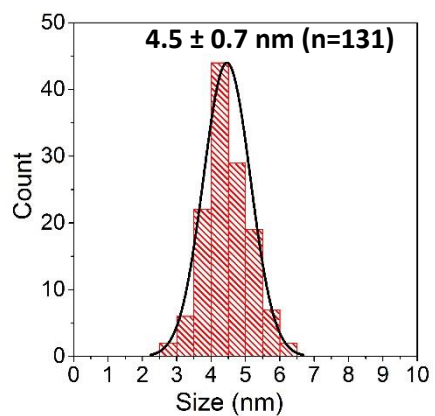
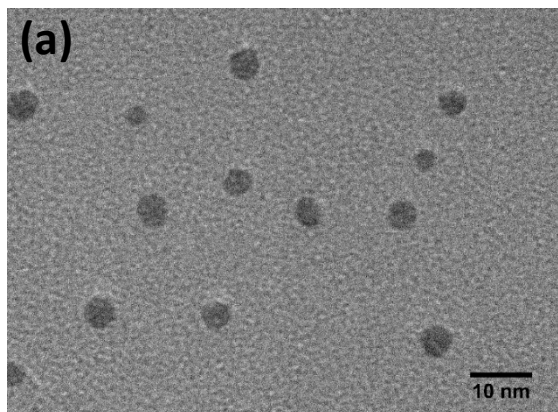


Figure S1 TEM images of 4.5 nm AuNPs (a), 15 nm AuNPs (b) and 26 nm AuNPs (c) with associated size distribution data.

Table S1 Full characterisation of as-synthesised AuNPs

Property	4.5 nm AuNPs	15 nm AuNPs	26 nm AuNPs
Surface plasmon peak	514 nm	519 nm	525 nm
Size by DLS	4.8 nm	21 nm	32 nm
Size by TEM	4.5 ± 0.7 nm	15 ± 2 nm	26 ± 3 nm
Concentration in ppm	125 mg/L	118 mg/L	189 mg/L
Number of AuNPs/mL	1.45×10 ¹⁴	3.83×10 ¹²	1.08×10 ¹²
Extinction Coefficient ³	1.67×10 ⁷ L mol ⁻¹ cm ⁻¹	3.03×10 ⁸ L mol ⁻¹ cm ⁻¹	2.72×10 ⁹ L mol ⁻¹ cm ⁻¹

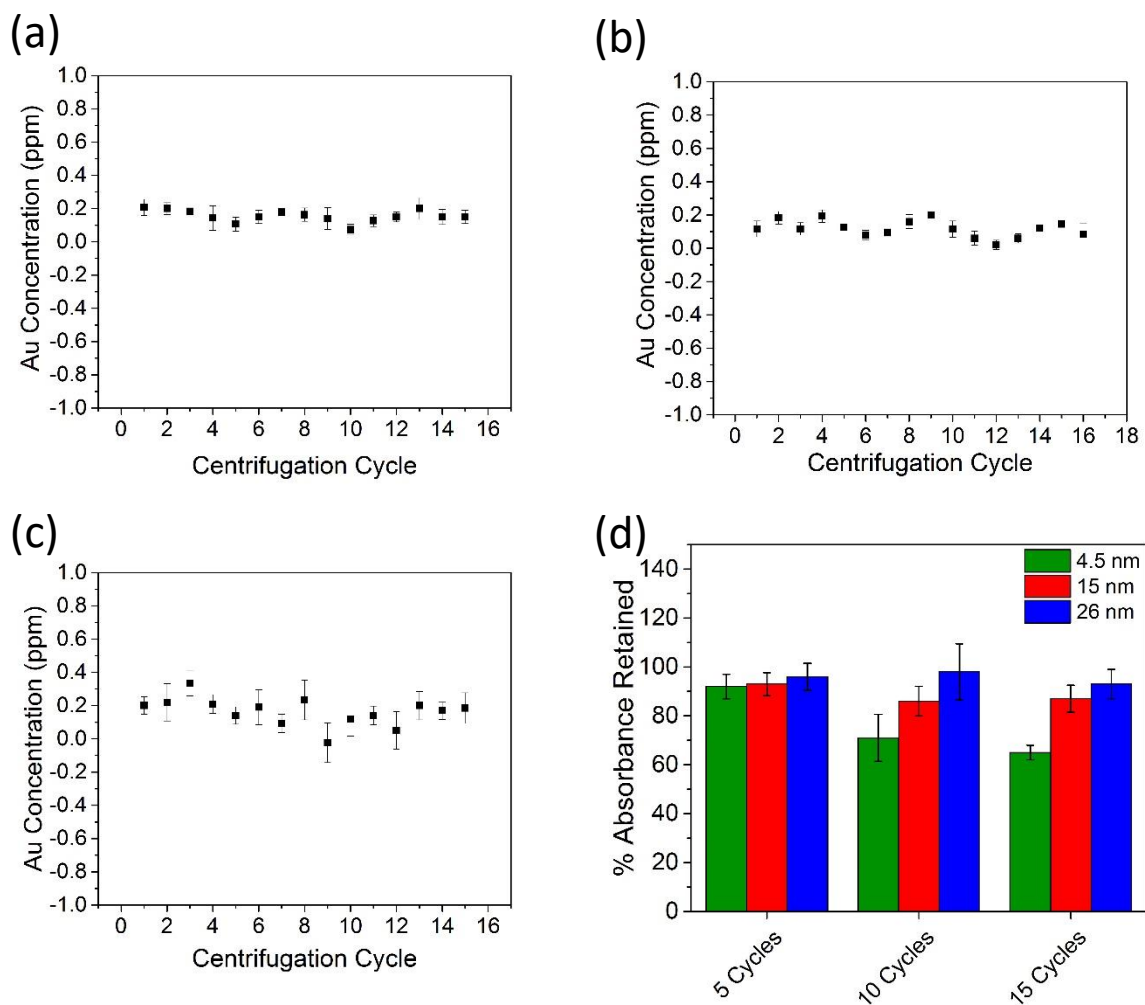
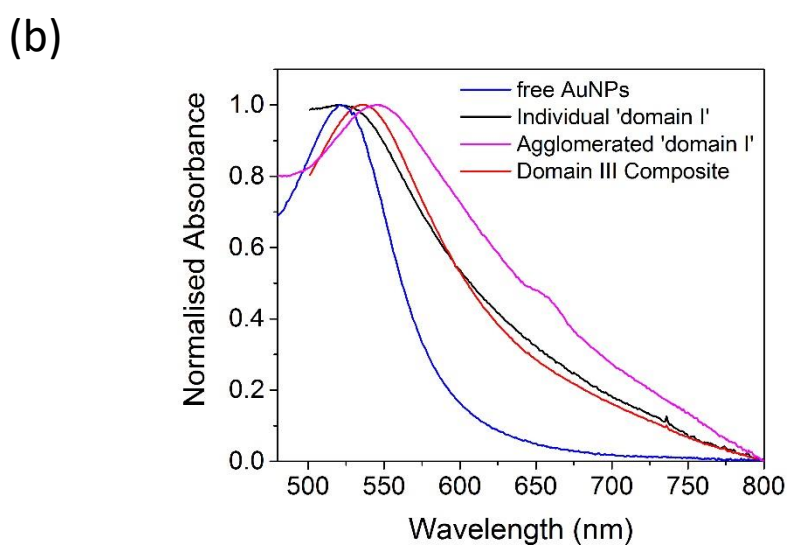
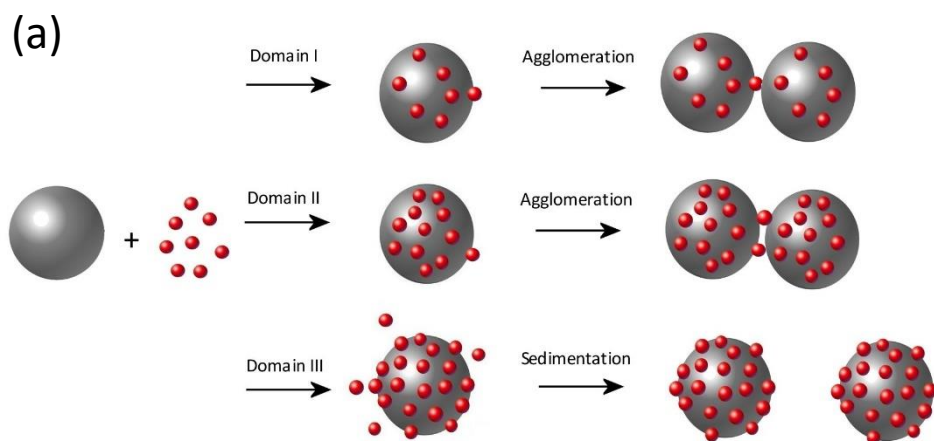


Figure S2 AAS measurements of the supernatant Au concentration for (a) 4.5 nm, (b) 15 nm and (c) 26 nm AuNPs@200 nm PS over 15 centrifugation-dispersion cycles. (d) A summary detailing the retention of optical absorbance as a function of centrifugation-dispersion cycles for the different composite families.

Table S2 Full characterisation of the 15 nm AuNP@200 nm PS composites

Max. Loading UV-Vis	Max. Loading AAS	Composite Loading AAS	DLS Δ nm	Zeta Potential Shift	% PS SA covered	SAPs per AuNP	% Au weight	AuNP SA per weight
124 \pm 5	138 \pm 3	131 \pm 11	51 nm	-45.9 mV	17.9 %	962 nm ²	50 %	10.5 m ² /g



(c)



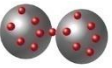

	Description	λ_{spr}	Stability	Redispersion Conditions
	unbound 15 nm AuNPs	519 nm	Fully Dispersed	n/a
	Individual 'Domain I' 15 nm AuNP@PS	521 nm	Agglomerate over time	Sonication at low conc.
	Agglomerated 'Domain I' 15 nm AuNP@PS	546 nm	Agglomerated	n/a
	'Domain III' 15 nm AuNP@PS	535 nm	Sediment over time	Mild sonication/ agitation

Figure S3 (a) Scheme showing the loading—dependent interactions of composite particles. (b) Normalised UV-Visible spectra showing the shift in the wavelength for different AuNPs populations of 15 nm AuNPs@200 nm PS. (c) Summary of the changes in optical properties and the loading-dependent dispersibility /stability of the composite particles.

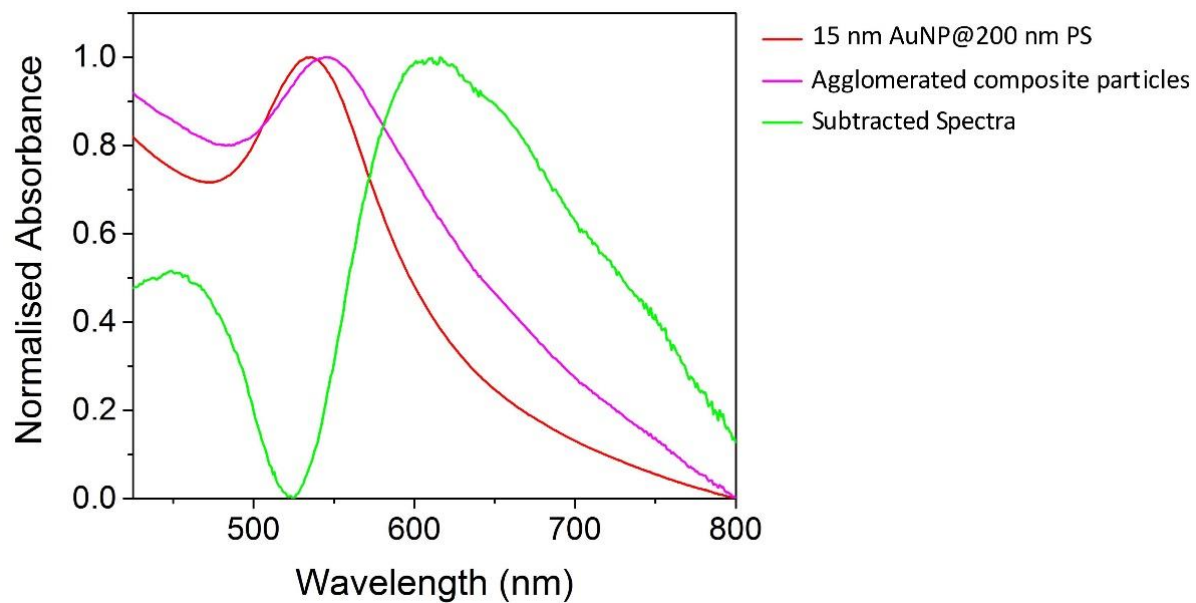


Figure S4 Normalized UV-visible absorbance spectra for both the discrete composite materials (domain III) and the agglomerated composite materials (domain I) as well as the subtraction of the discrete spectra from the agglomerated spectra.

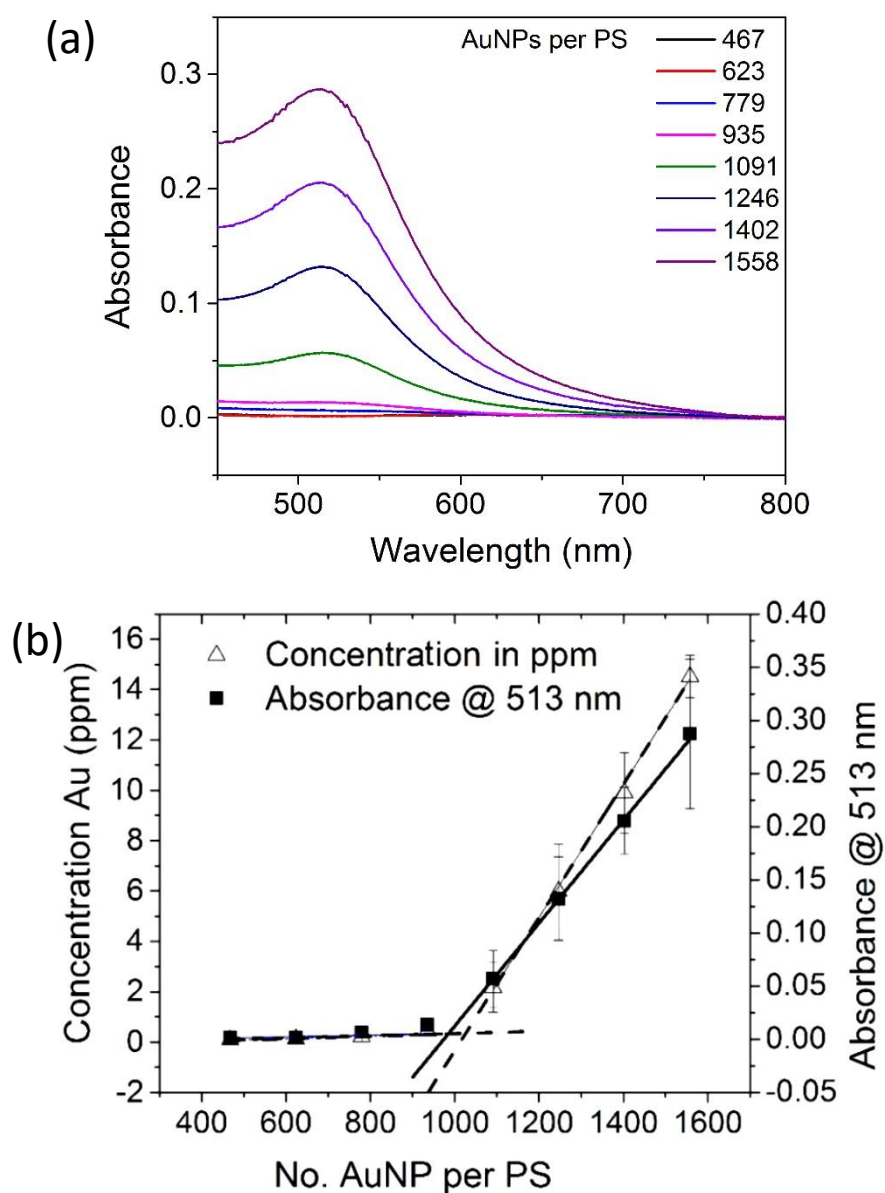


Figure S5 (a) UV-visible spectra of supernatant containing excess unbound AuNPs. (b) Determination of the maximum loading of the 4.5 nm AuNPs on the 200 nm PS beads by UV-visible (solid line) and atomic absorption spectroscopy (dashed line). The two intercepts indicate the point of saturation of gold nanoparticles on the surface of the PS bead. All measurements were done in triplicate on the supernatant of three different batches in aqueous solution.

Table S3 Full characterisation of the 4.5 nm AuNP@200 nm PS composites

Max. Loading UV-Vis	Max. Loading AAS	Composite Loading AAS	DLS Δ nm	Zeta Potential Shift	% PS SA covered	SA _{PS} per AuNP	% Au weight	AuNP SA per weight
977 ± 6	1015 ± 11	978 ± 48	15 nm	-38 mV	12.5 %	127 nm ²	17 %	11.8 m ² /g

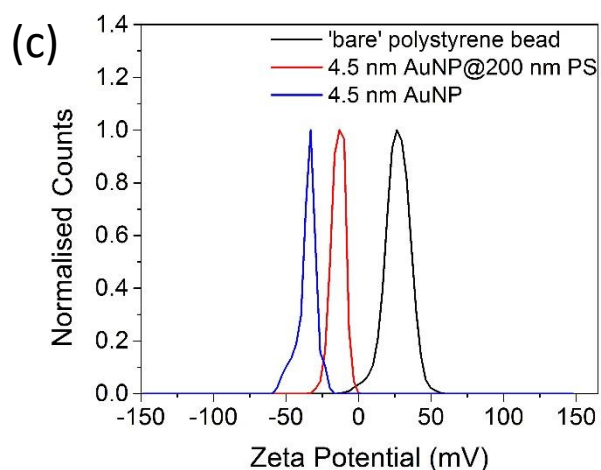
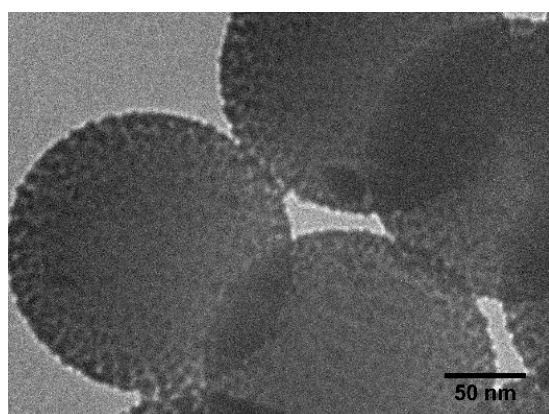
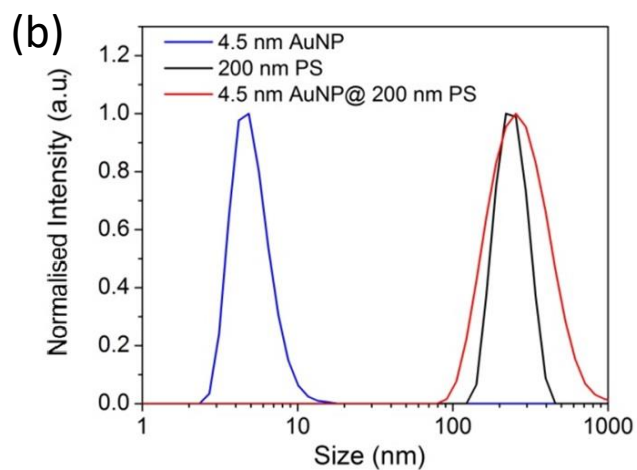
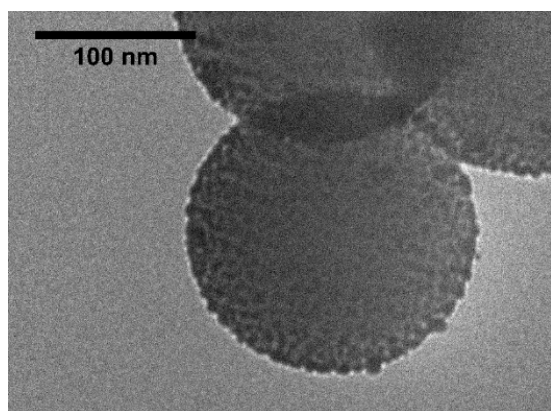
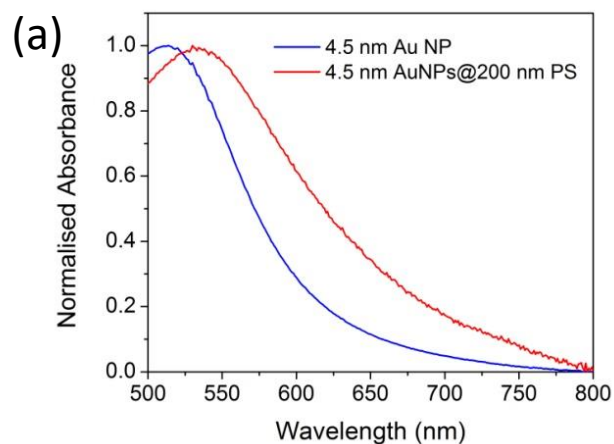
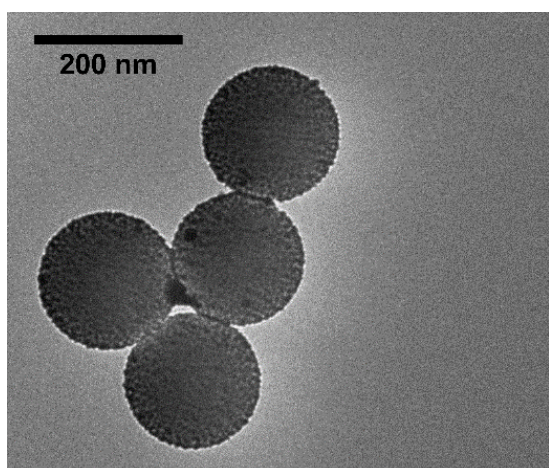


Figure S6 (left) TEM images of 4.5 nm AuNP@200 nm PS composite materials. (a) UV-visible data of 4.5 nm AuNP and 4.5 nm AuNP@200 nm PS composite particles, (b) dynamic light scattering of 4.5 nm AuNPs, 200 nm PS beads and 4.5 nm AuNP@200 nm PS composite particles and (c) zeta potential data for 200 nm PS, 4.5 nm AuNPs and 4.5 nm AuNP@200 nm PS composite particles all in aqueous solution (pH 7.4).

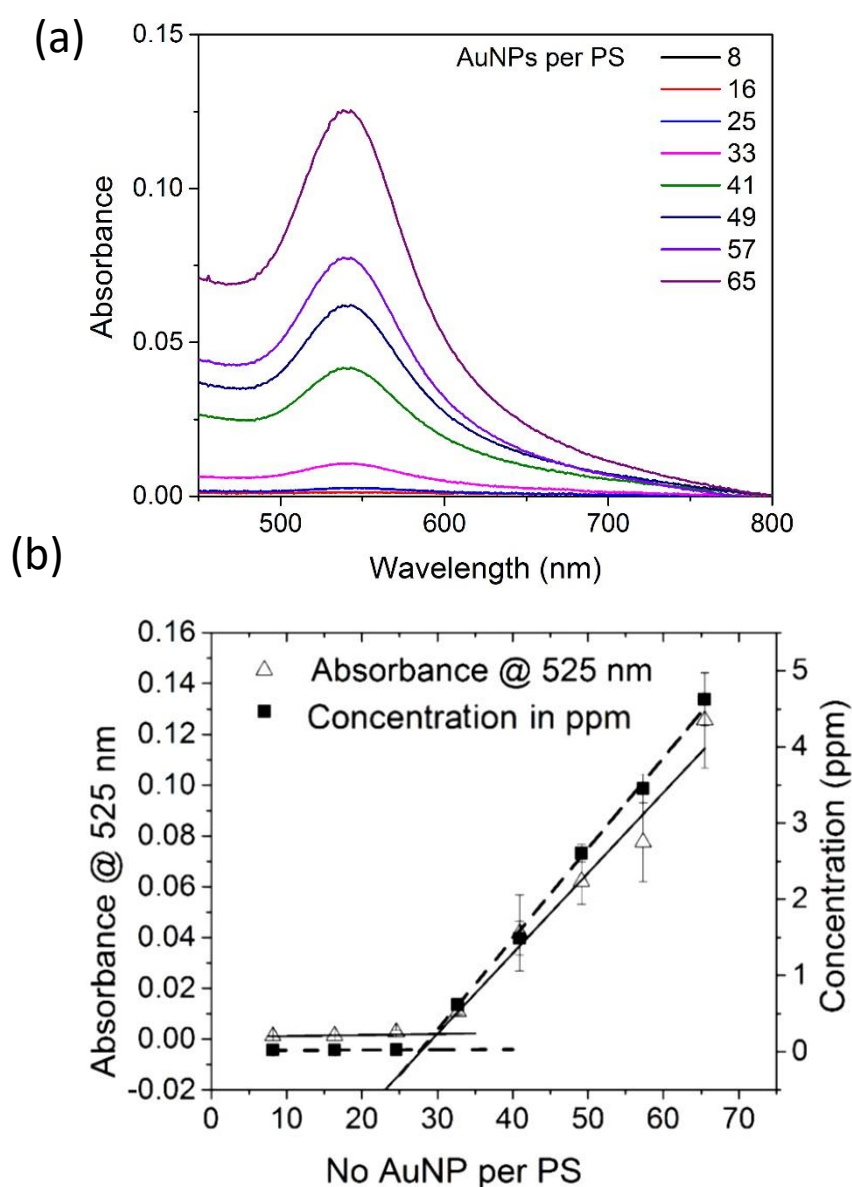


Figure S7 (a) UV-visible spectra of supernatant containing excess unbound AuNPs. (b) Determination of the maximum loading of the 26 nm AuNPs on the 200 nm PS beads by UV-visible (solid line) and atomic absorption spectroscopy (dashed line). The two intercepts indicate the point of saturation of gold nanoparticles on the surface of the PS bead. All measurements were done in triplicate on the supernatant of three different batches in aqueous solution.

Table S4 Full characterisation of the 26 nm AuNP@200 nm PS composites

Max. Loading UV-Vis	Max. Loading AAS	Composite Loading AAS	DLS Δ nm	Zeta Potential Shift	% PS SA covered	SA _{ps} per AuNP	% Au weight	AuNP SA per weight
30 ± 2	28 ± 1	32 ± 3	85 nm	-34 mV	12.7 %	4200 nm ²	55 %	6.5 m ² /g

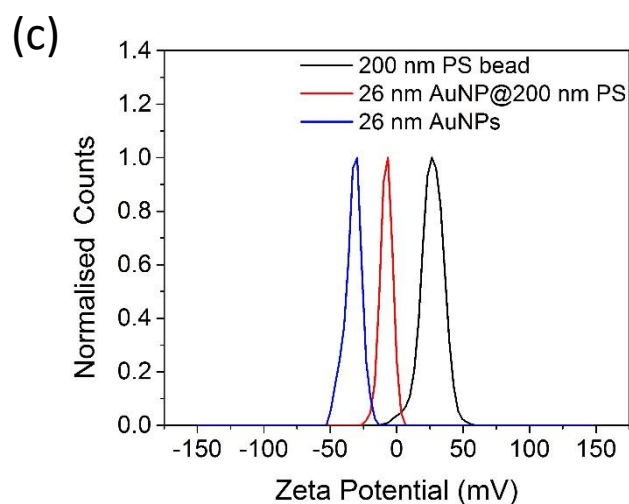
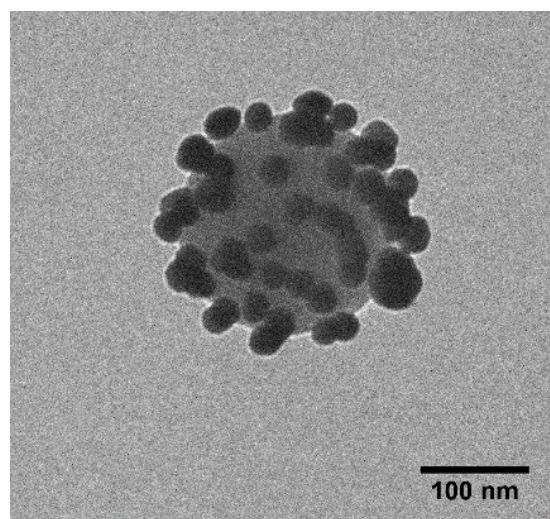
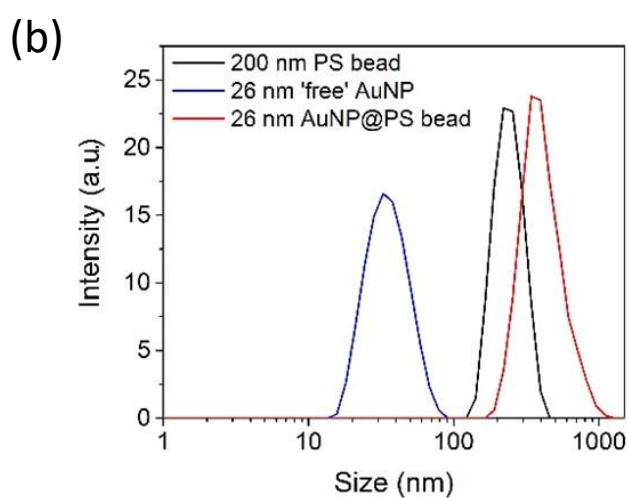
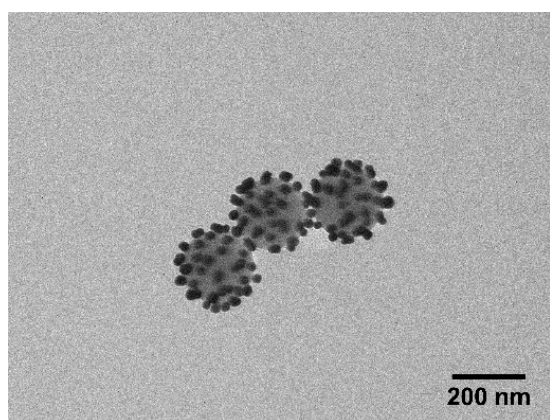
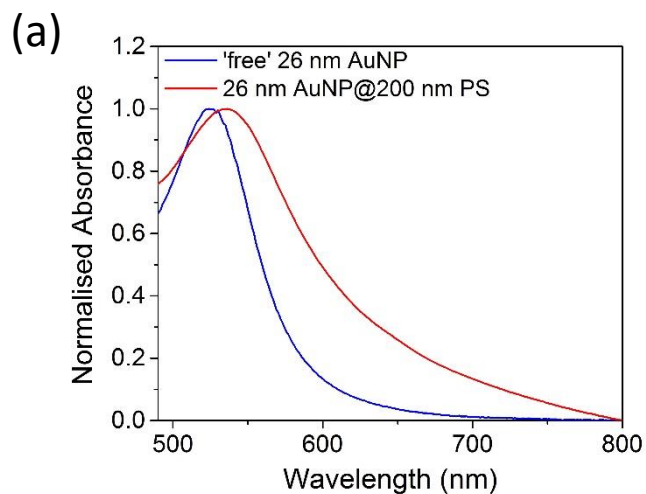
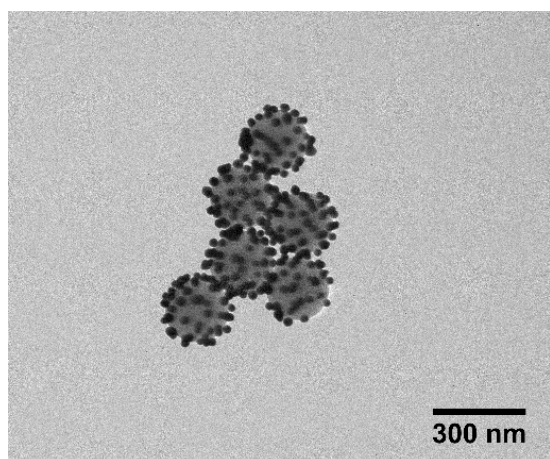


Figure S8 (left) TEM images of 26 nm AuNP@200 nm PS composite materials. (a) UV-visible data of 26 nm AuNP and 26 nm AuNP@200 nm PS composite particles, (b) dynamic light scattering of 26 nm AuNPs, 200 nm PS beads and 26 nm AuNP@200 nm PS composite and (c) zeta potential (pH 7) data for the 200 nm PS, 26 nm AuNPs and 26 nm AuNP@200 nm PS composite, all in aqueous solution (pH 7.4).

Table S5 Summary of the composite loading properties

AuNP@PS Bead	Max. Loading UV-Vis	Max. Loading AAS	Composite Loading AAS	% PS SA covered	SA_{PS} per AuNP	% Au weight	AuNP SA per weight
15 nm@200nm	124 ± 5	138 ± 3	131 ± 11	17.9 %	962 nm ²	50 %	10.5 m ² /g
4.5 nm@200nm	977 ± 6	1015 ± 11	978 ± 48	12.5 %	127 nm ²	17 %	11.8 m ² /g
26 nm@200nm	30 ± 2	28 ± 1	32 ± 3	12.7 %	4200 nm ²	55 %	6.5 m ² /g
15nm @2000nm	7429 ± 273	7211 ± 183	7622 ± 453	10.4%	1693 nm ²	6 %	1.12 m ² /g

Table S6 Optical properties of composite particles

AuNP@PS Bead	λ₀ (original SPR)	Δλ (shift in SPR)
4.5 nm@200 nm	514 nm	16 nm
15 nm@200 nm	519 nm	16 nm
26 nm@200 nm	525 nm	13 nm
15 nm@2000 nm	519 nm	14 nm

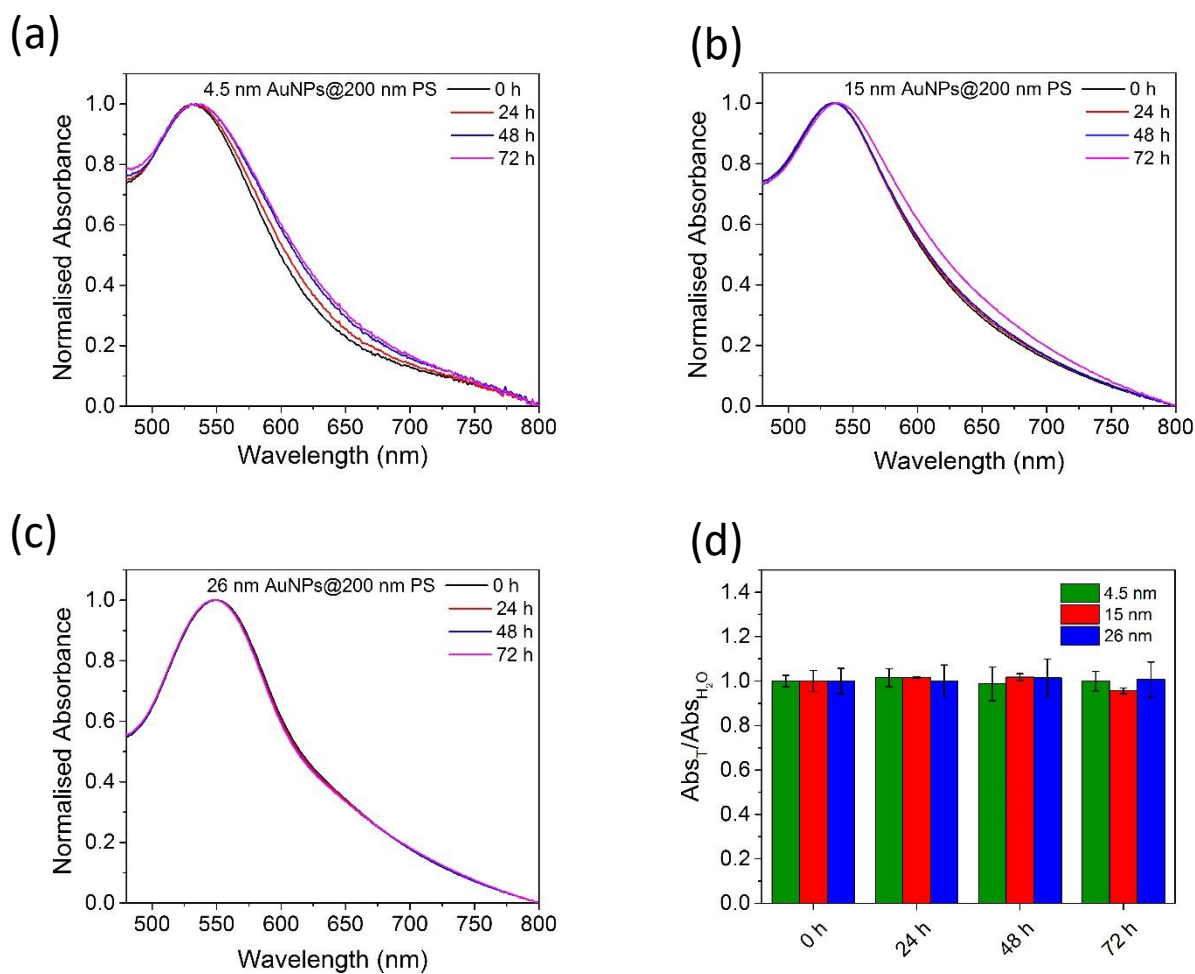


Figure S9 Normalized UV-visible spectra of (a) 4.5 nm, (b) 15 nm and (c) 26 nm AuNPs@200 nm PS in H₂O at different time points and (d) graph showing retention of optical absorbance as a function of time for each family

Table S7 Summary of SPR shift of composite particles at different time points in H₂O

AuNP@PS Bead	$\Delta\lambda$ 0 h	$\Delta\lambda$ 24 h	$\Delta\lambda$ 48 h	$\Delta\lambda$ 72 h
4.5 nm@200 nm	0 nm	0 nm	0 nm	0 nm
15 nm@200 nm	0 nm	0 nm	0 nm	4 nm
26 nm@200 nm	0 nm	0 nm	0 nm	0 nm

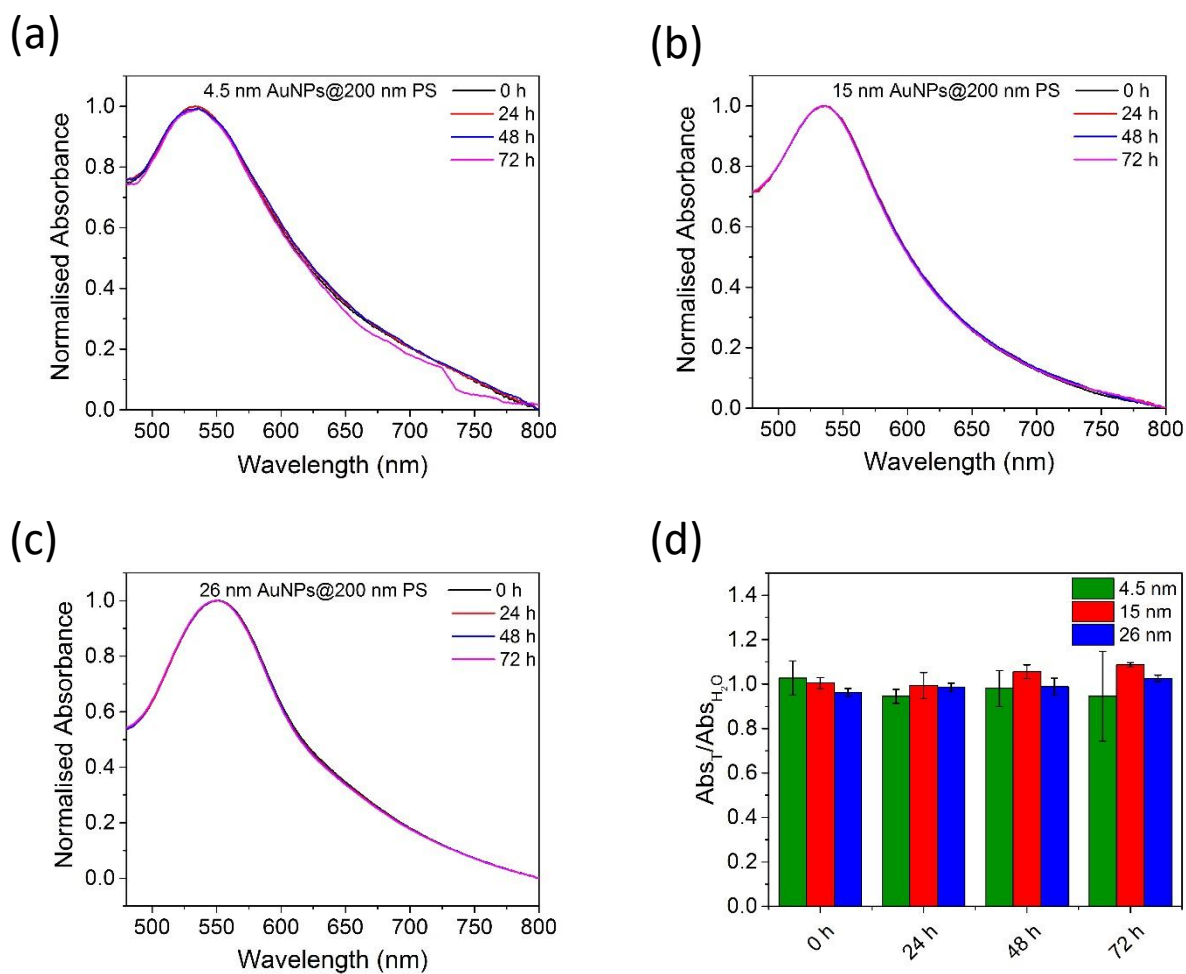


Figure S10 Normalized UV-visible spectra of (a) 4.5 nm, (b) 15 nm and (c) 26 nm AuNPs@200 nm PS in 70 % ethanol at different time points and (d) graph showing retention of optical absorbance as a function of time for each family

Table S8 Summary of SPR shift of composite particles at different time points in 70 % EtOH

AuNP@PS Bead	$\Delta\lambda$ 0 h	$\Delta\lambda$ 24 h	$\Delta\lambda$ 48 h	$\Delta\lambda$ 72 h
4.5 nm@200 nm	2 nm	5 nm	5 nm	3 nm
15 nm@200 nm	0 nm	0 nm	0 nm	3 nm
26 nm@200 nm	5 nm	5 nm	5 nm	2 nm

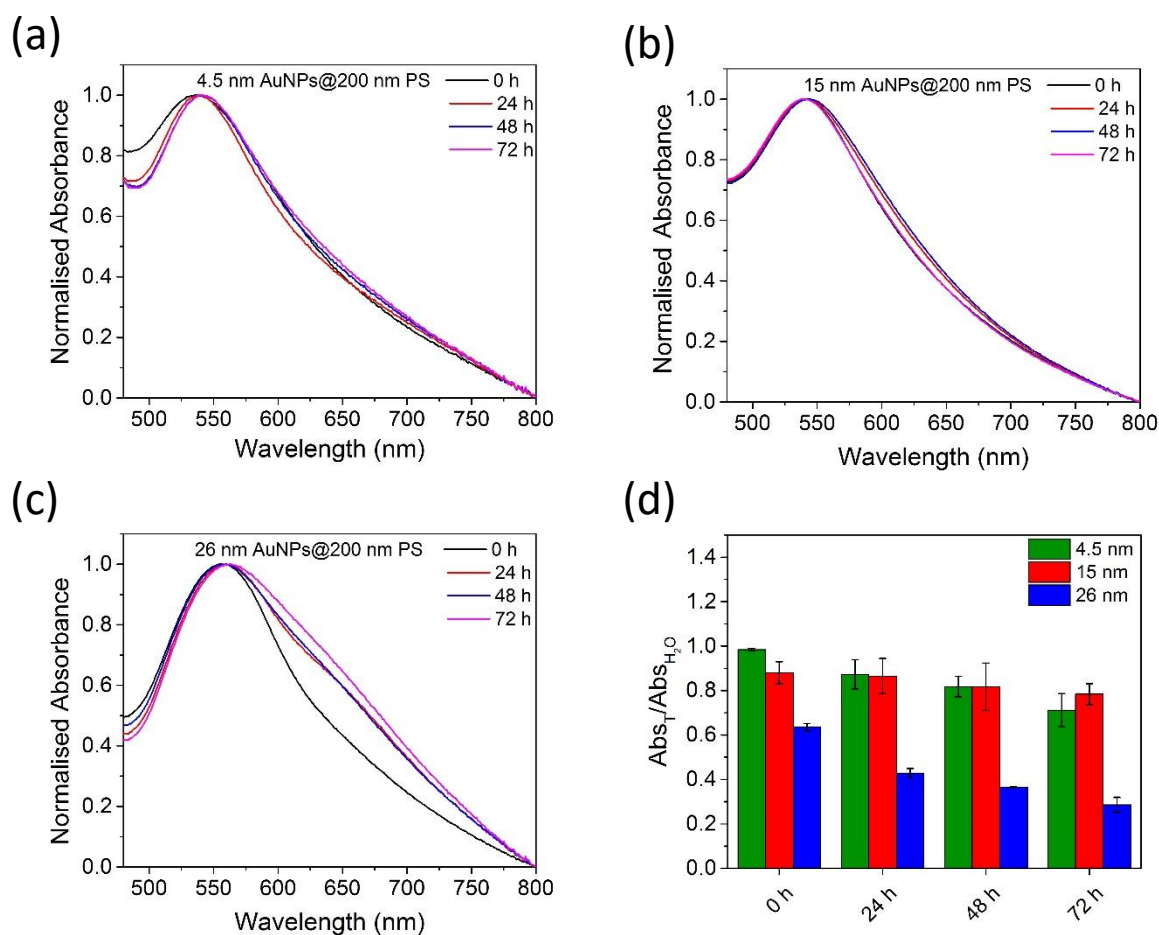


Figure S11 Normalised UV-visible spectra of (a) 4.5 nm, (b) 15 nm and (c) 26 nm AuNPs@200 nm PS in 250 mM NaCl at different time points and (d) graph showing retention of optical absorbance as a function of time for each family.

Table S9 Summary of SPR shift of composite particles at different time points in 250 mM NaCl

AuNP@PS Bead	$\Delta\lambda$	$\Delta\lambda$	$\Delta\lambda$	$\Delta\lambda$
	0 h	24 h	48 h	72 h
4.5 nm@200 nm	5 nm	5 nm	11 nm	10 nm
15 nm@200 nm	5 nm	7 nm	10 nm	10 nm
26 nm@200 nm	7 nm	11 nm	11 nm	13 nm

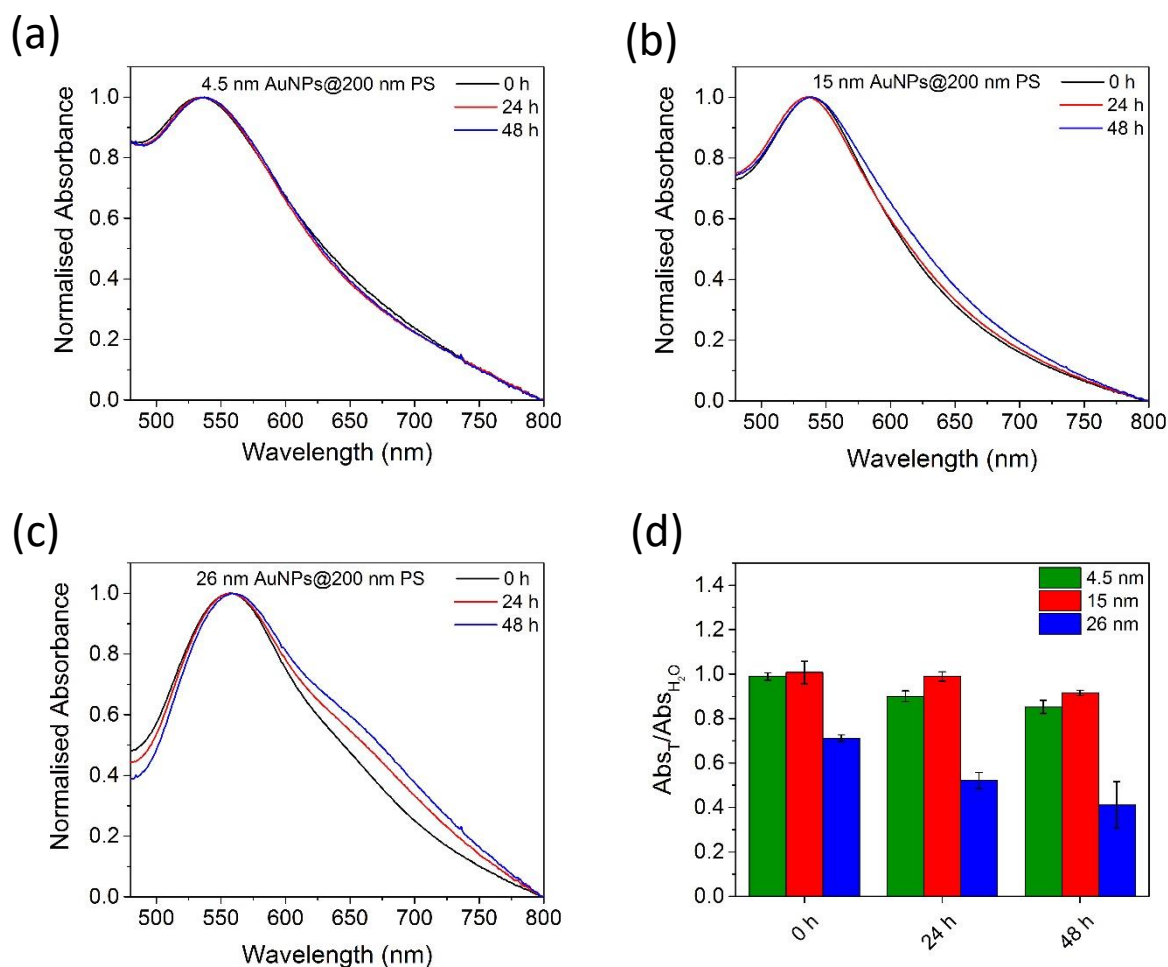


Figure S12 Normalised UV-visible spectra of (a) 4.5 nm, (b) 15 nm and (c) 26 nm AuNPs@200 nm PS in 350 mM NaCl at different time points and (d) graph showing retention of optical absorbance as a function of time for each family.

Table S10 Summary of SPR shift of composite particles at different time points in 350 mM NaCl

AuNP@PS Bead	$\Delta\lambda$	$\Delta\lambda$	$\Delta\lambda$
	0 h	24 h	48 h
4.5 nm@200 nm	0 nm	6 nm	11 nm
15 nm@200 nm	5 nm	11 nm	11 nm
26 nm@200 nm	8 nm	9 nm	10 nm

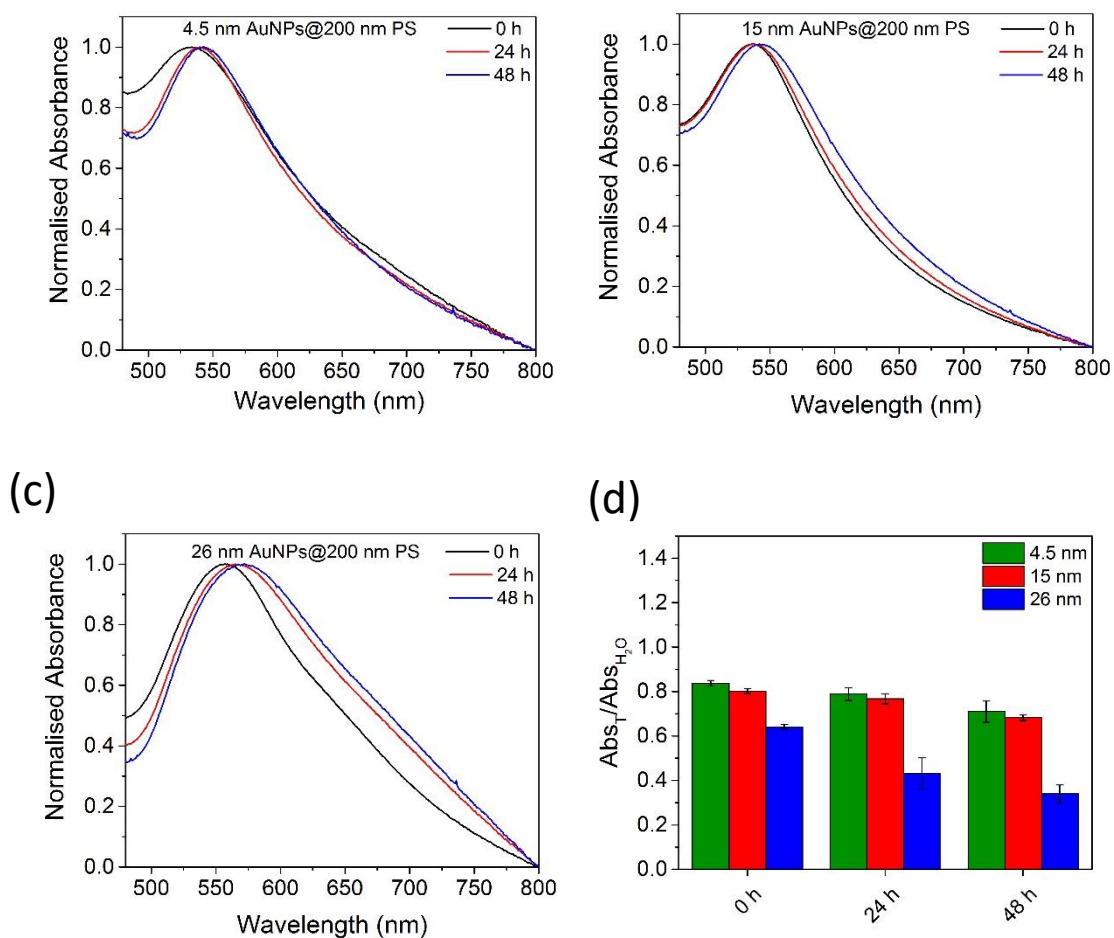


Figure S13 Normalised UV-visible spectra of (a) 4.5 nm, (b) 15 nm and (c) 26 nm AuNPs@200 nm PS in 500 mM NaCl at different time points and (d) graph showing retention of optical absorbance as a function of time for each family.

Table S11 Summary of SPR shift of composite particles at different time points in 500 mM NaCl

AuNP@PS Bead	$\Delta\lambda$	$\Delta\lambda$	$\Delta\lambda$
	0 h	24 h	48 h
4.5 nm@200 nm	4 nm	10 nm	12 nm
15 nm@200 nm	5 nm	13 nm	11 nm
26 nm@200 nm	10 nm	16 nm	23 nm

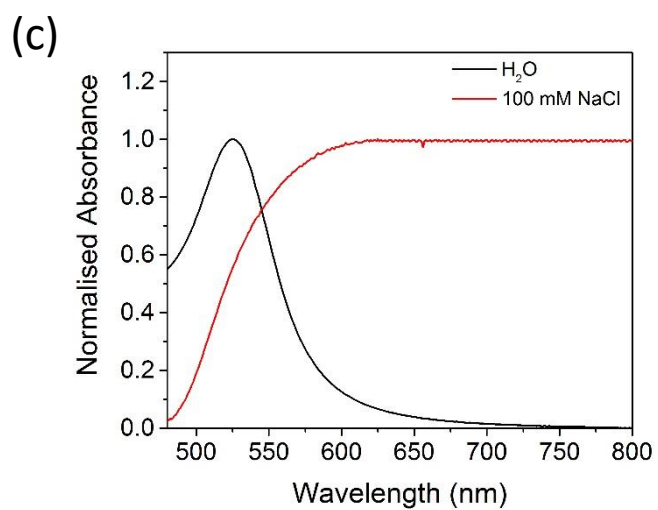
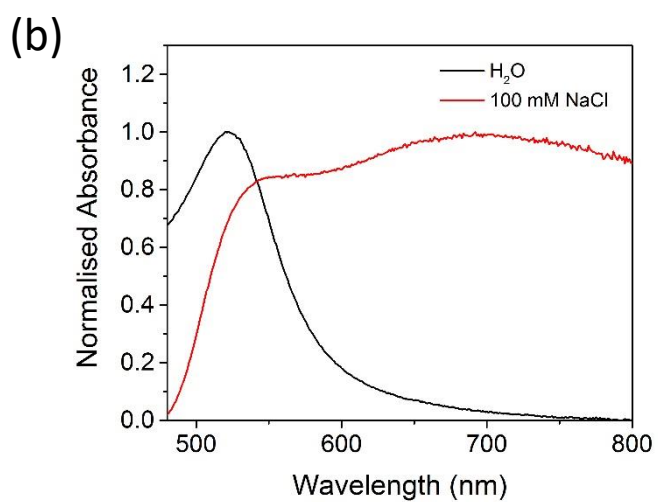
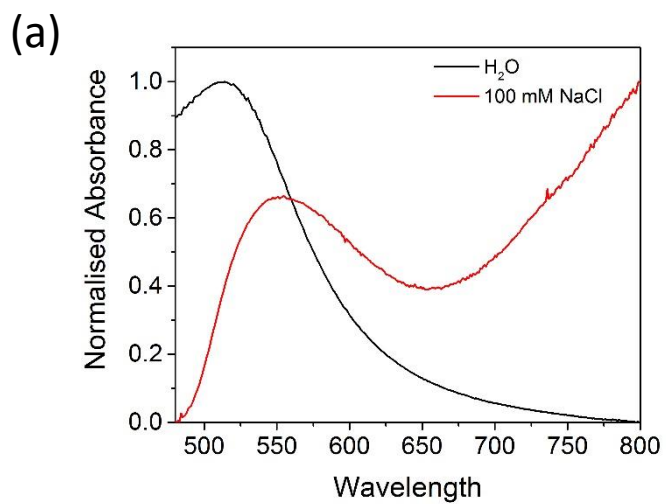


Figure S14 Normalized UV-Visible spectra of (a) 4.5 nm, (b) 15 nm and (c) 26 nm AuNPs in both H₂O and 100 mM NaCl

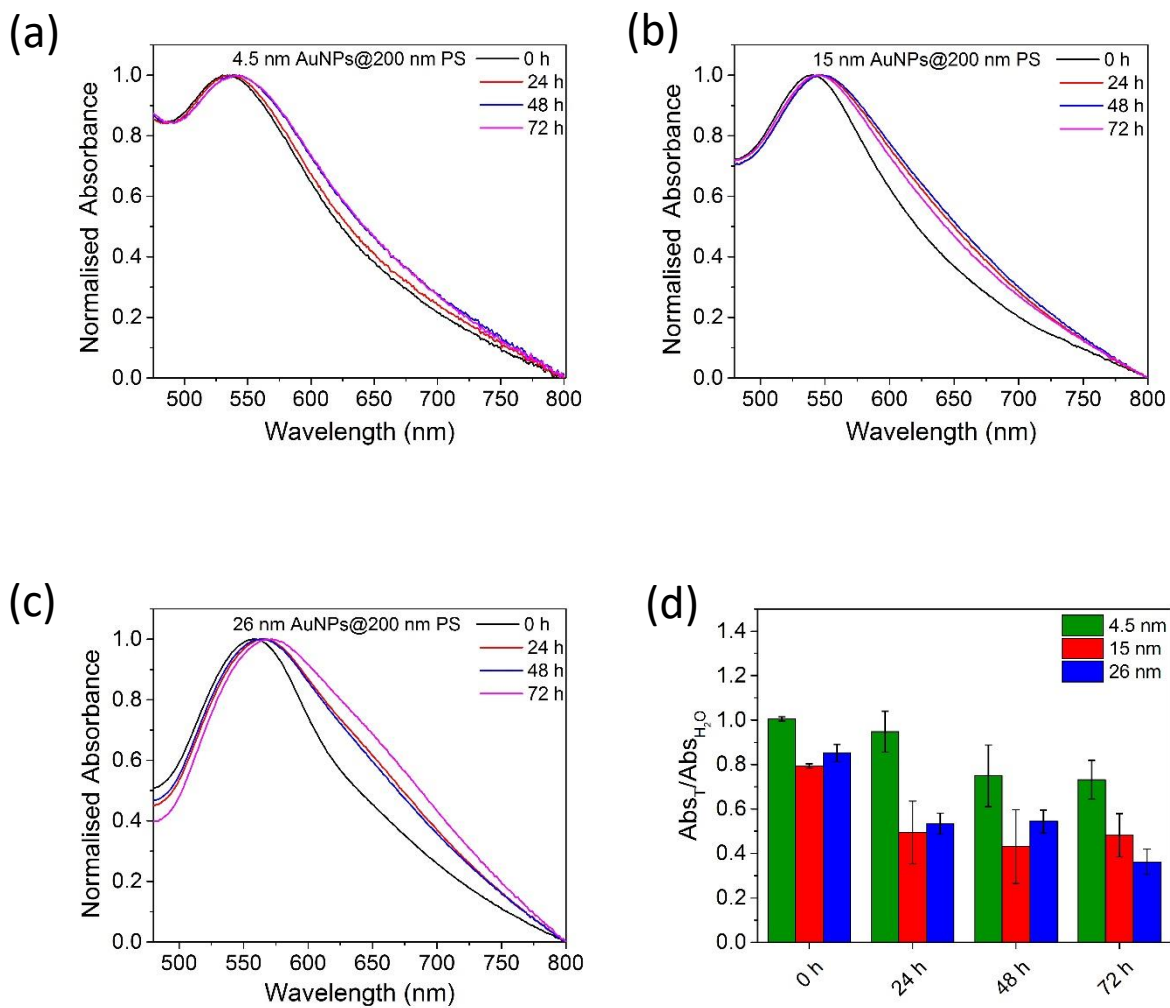


Figure S15 Normalised UV-visible spectra of (a) 4.5 nm, (b) 15 nm and (c) 26 nm AuNPs@200 nm PS in 10 mM PBS at different time points and (d) graph showing retention of optical absorbance as a function of time for each family.

Table S12 Summary of SPR shift of composite particles at different time points in 10 mM PBS

AuNP@PS Bead	$\Delta\lambda$	$\Delta\lambda$	$\Delta\lambda$	$\Delta\lambda$
	0 h	24 h	48 h	72 h
4.5 nm@200 nm	0 nm	6 nm	11 nm	11 nm
15 nm@200 nm	5 nm	11 nm	11 nm	11 nm
26 nm@200 nm	15 nm	15 nm	12 nm	13 nm

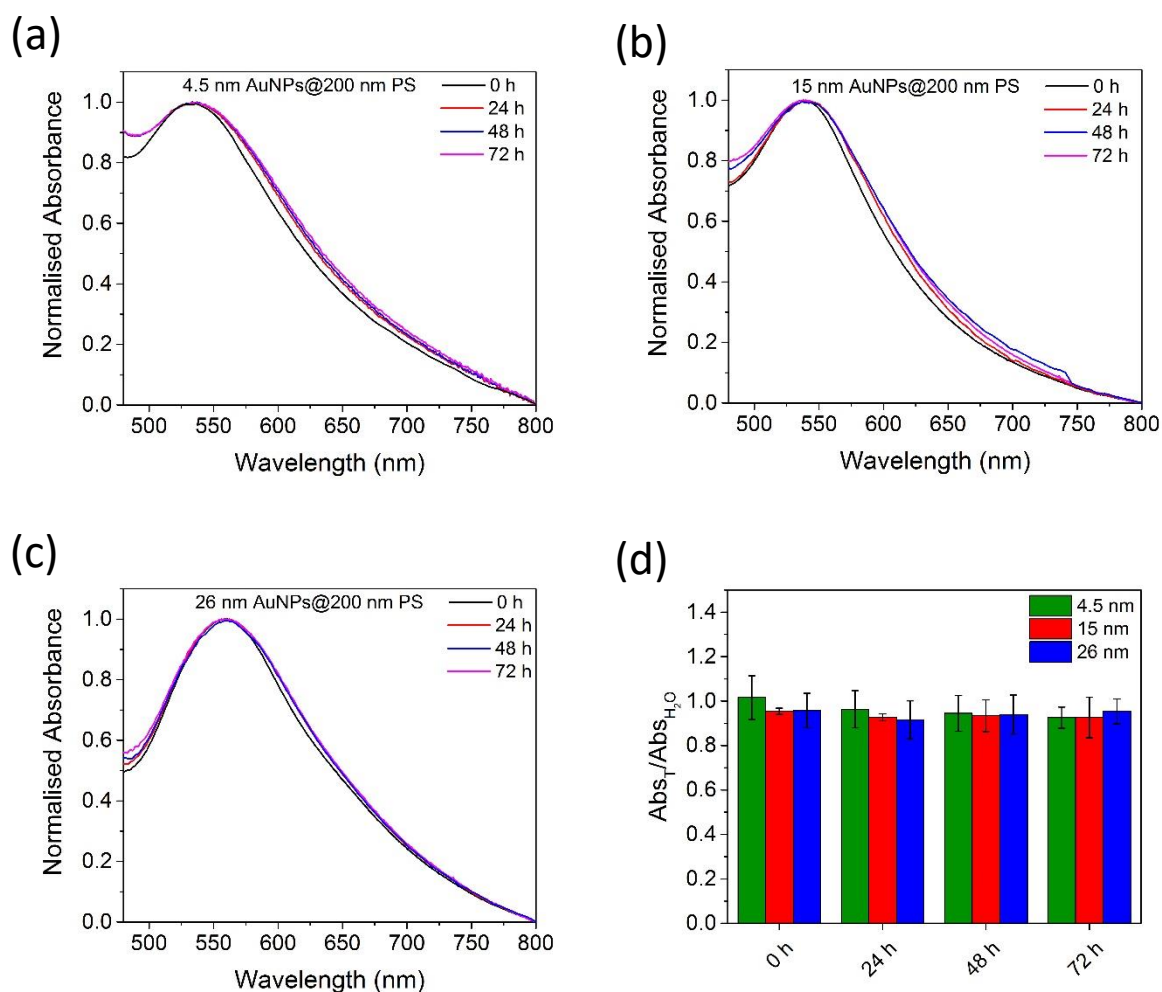


Figure S16 Normalised UV-visible spectra of (a) 4.5 nm, (b) 15 nm and (c) 26 nm AuNPs@200 nm PS in DMEM supplemented with 10 % FBS at different time points and (d) graph showing retention of optical absorbance as a function of time for each family.

Table S13 Summary of SPR shift of composite particles at different time points in DMEM supplemented with 10 % FBS

AuNP@PS Bead	$\Delta\lambda$	$\Delta\lambda$	$\Delta\lambda$	$\Delta\lambda$
	0 h	24 h	48 h	72 h
4.5 nm@200 nm	5 nm	6 nm	6 nm	6 nm
15 nm@200 nm	3 nm	3 nm	3 nm	3 nm
26 nm@200 nm	11 nm	9 nm	9 nm	11 nm

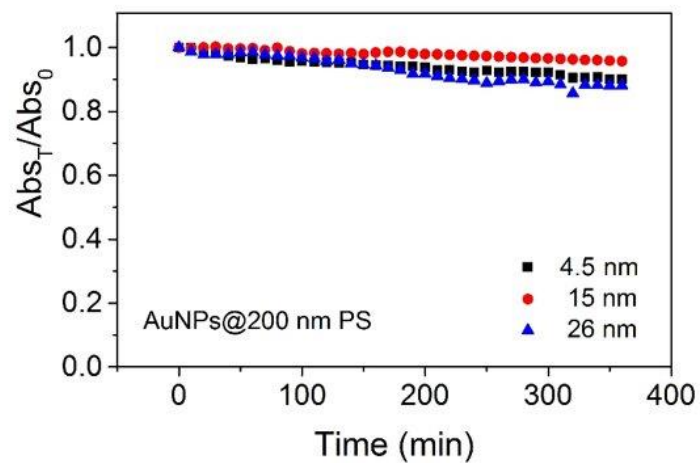


Figure S17 Graph showing the stability of composite families in DMEM supplemented with 10 % FBS over 360 min.

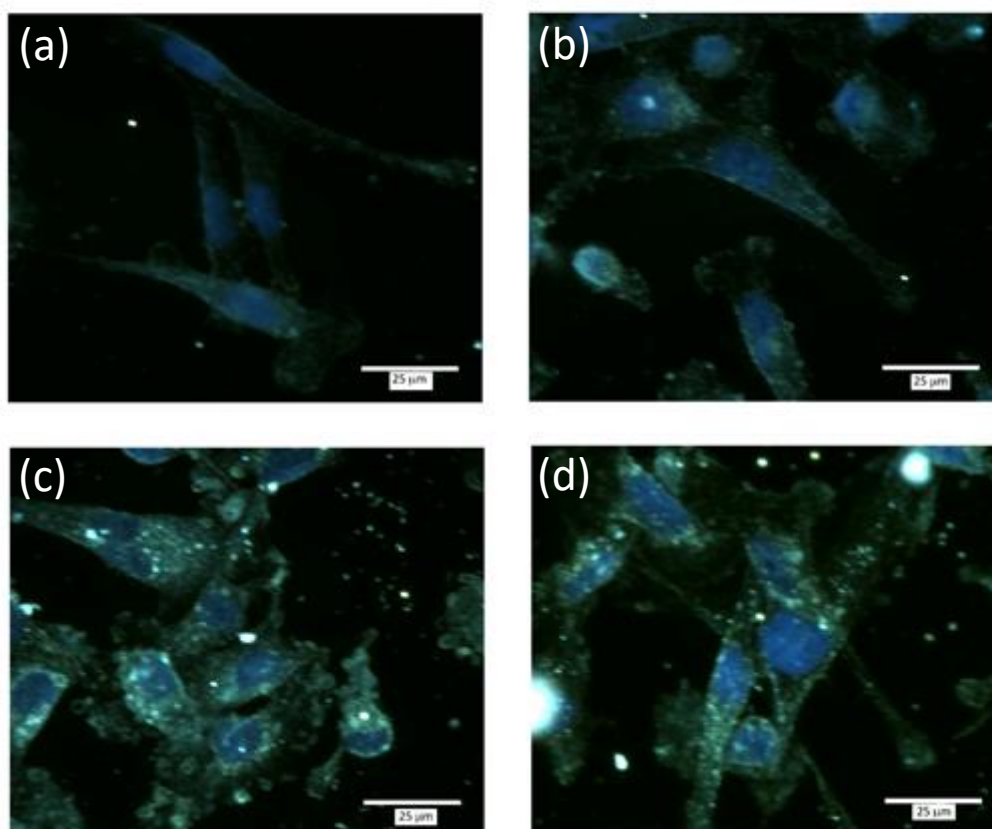


Figure S18 Enhanced fluorescence darkfield optical images of human breast adenocarcinoma cells (a,b) stained with DAPI and (c,d) incubated with 4.5 AuNP@200 nm PS for 6 h and stained with DAPI.

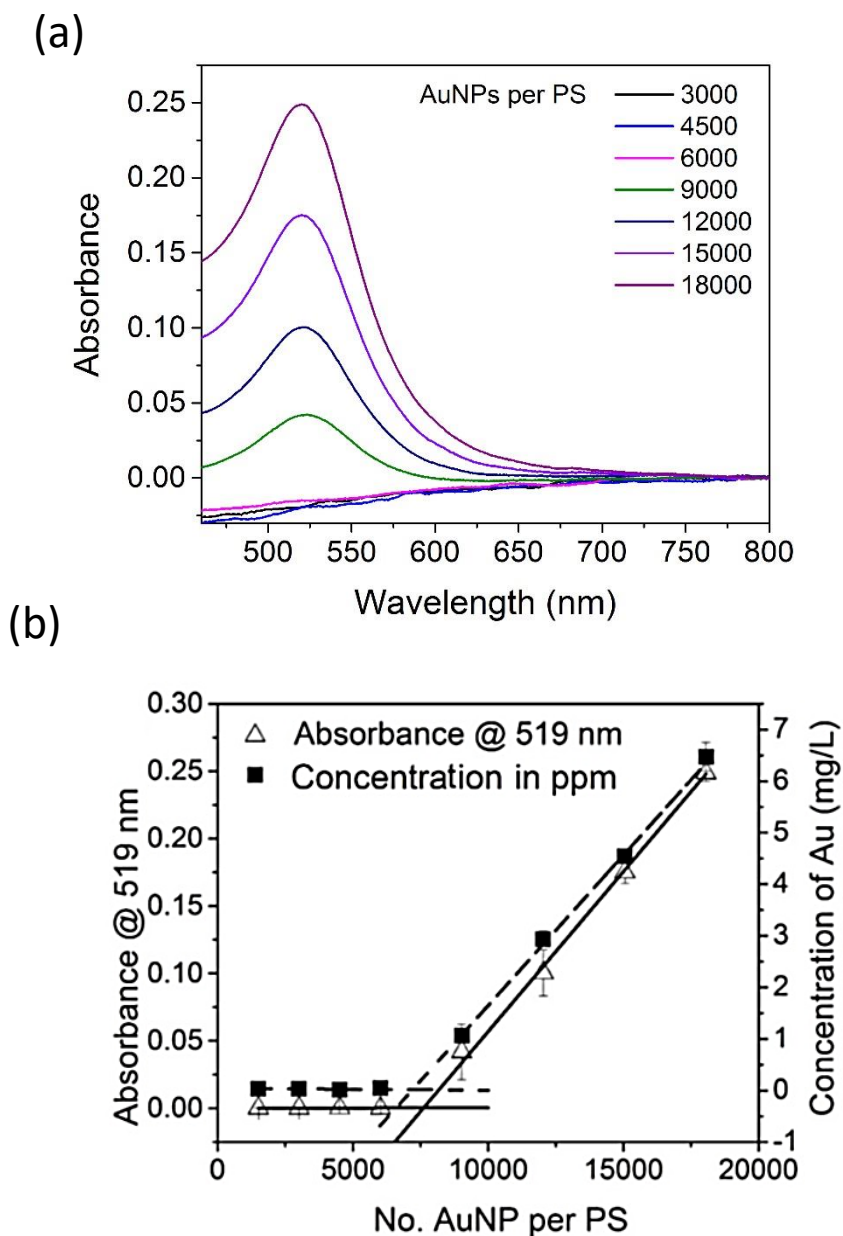


Figure S19 (a) UV-visible spectra of supernatant containing excess AuNPs. (b) Determination of the maximum loading of the 15 nm AuNPs on the 2000 nm PS beads. by UV-visible (solid line) and atomic absorption spectroscopy (dashed line). The two intercepts indicate the point of saturation of gold nanoparticles on the surface of the PS bead. All measurements were done in triplicate on the supernatant of three different batches in aqueous solution.

Table S14 Full characterisation of the 15 nm AuNP@2000 nm PS composites

Max. Loading UV-Vis	Max. Loading AAS	Composite Loading AAS	Zeta Potential Shift	% PS SA covered	SA _{PS} per AuNP	% Au weight	AuNP SA per weight
7429 ± 273	7211 ± 183	7622 ± 453	-26 mV	10.4%	1693 nm ²	6 %	1.12 m ² /g

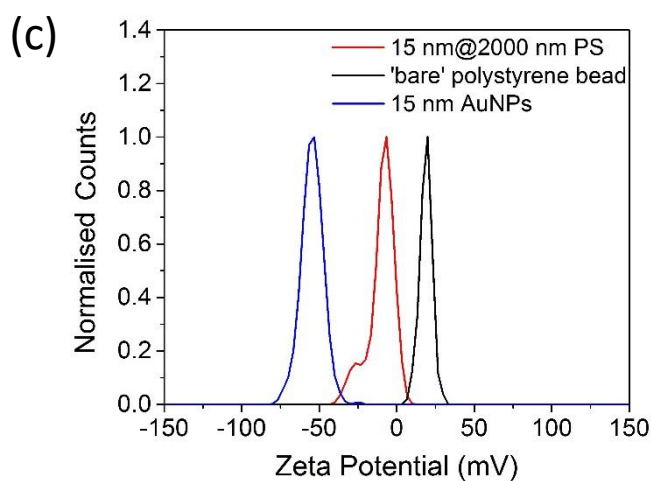
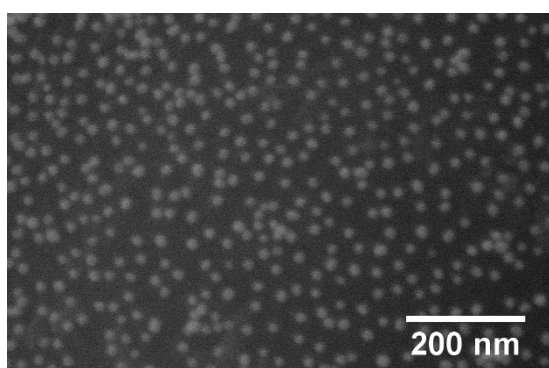
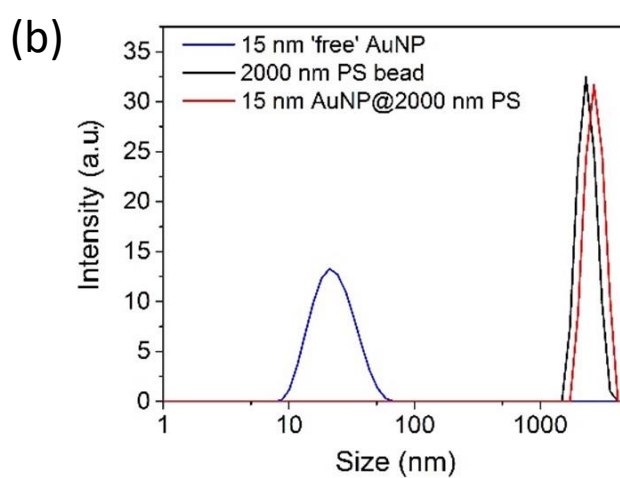
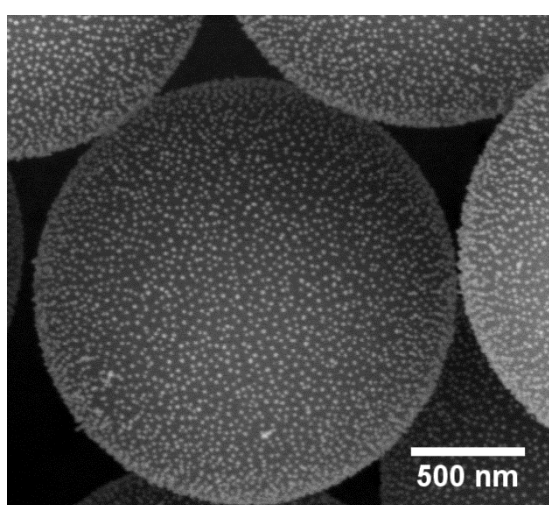
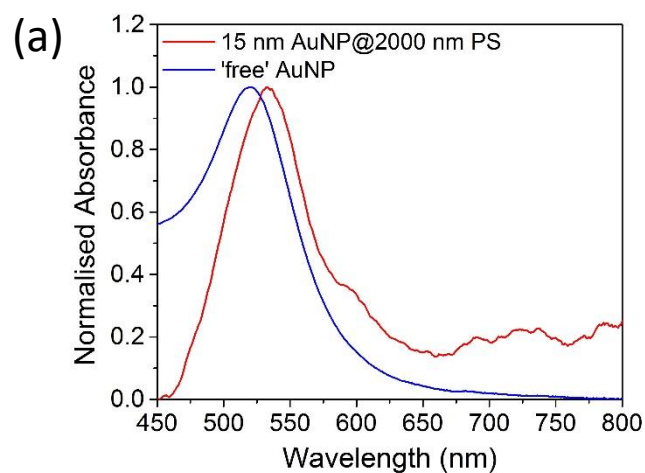
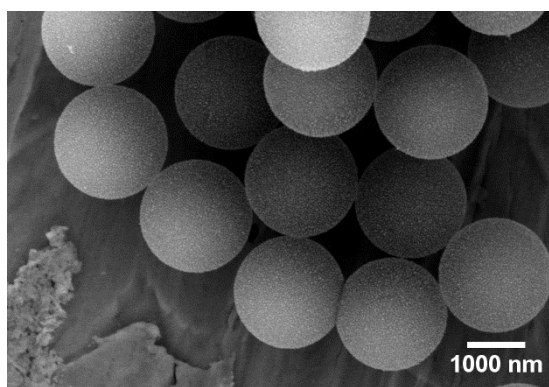


Figure S20 (left) SEM images of 15 nm AuNP@2000 nm PS composite materials. (a) UV-visible data of 15 nm AuNP and 15 nm AuNP@2000 nm PS composite particles, (b) dynamic light scattering of 15 nm AuNPs, 2000 nm PS beads and 15 nm AuNP@2000 nm PS composite and (c) zeta potential data for the 2000 nm PS, 15 nm AuNPs and 15 nm AuNP@2000 nm PS composite all in aqueous solution (pH 7.4).

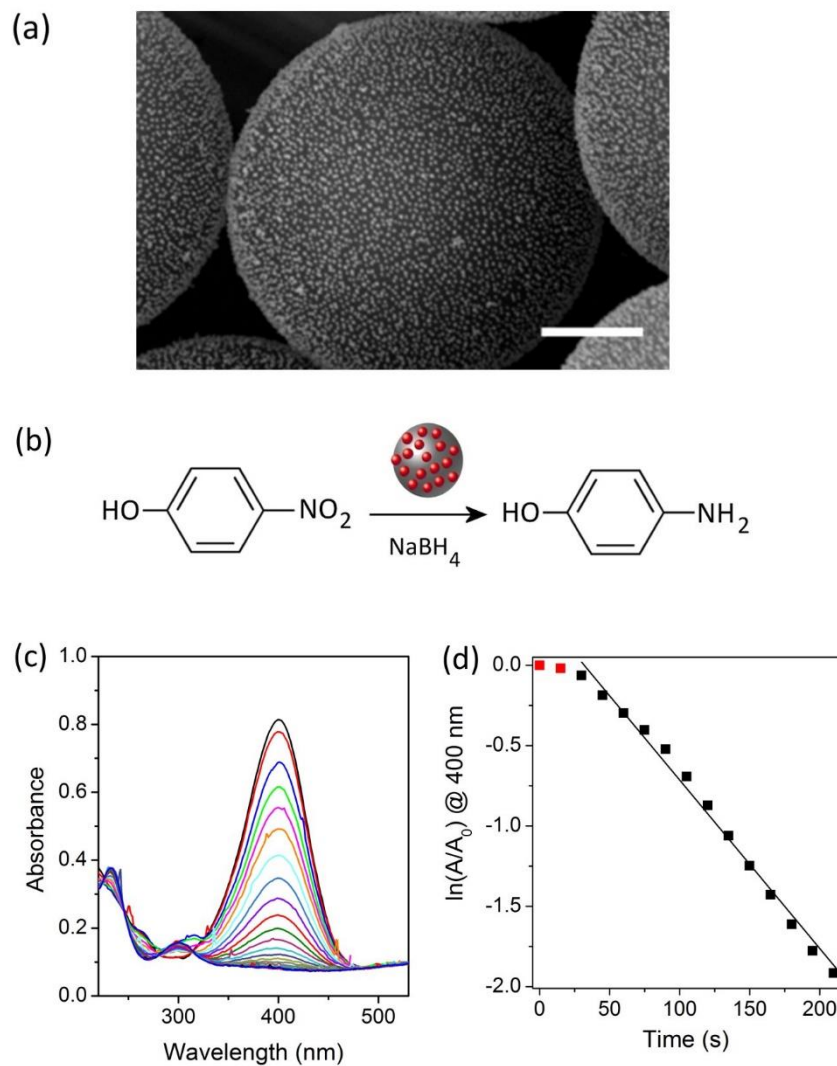


Figure S21 (a) SEM image of 15 nm AuNP@2000 nm PS (scale bar = 500 nm). (b) Reaction scheme showing the reduction of 4-nitrophenol in the presence of the 15 nm AuNP@2000 nm PS. (c) UV-visible spectra monitoring the reduction of 4-nitrophenol. (d) Kinetic fit of the natural log of A/A_0 at 400 nm vs. time (s).⁴

References

- 1 N. Jana, L. Gearheart and C. Murphy, *Langmuir*, 2001, **17**, 6782–6786.
- 2 N. G. Bastús, J. Comenge and V. Puntes, *Langmuir*, 2011, **27**, 11098–11105.
- 3 X. Liu, M. Atwater, J. Wang and Q. Huo, *Colloids Surfaces B Biointerfaces*, 2007, **58**, 3–7.
- 4 S. Panigrahi, S. Basu, S. Praharaj, S. Pande, S. Jana, A. Pal, S. K. Ghosh and T. Pal, *J. Phys. Chem. C*, 2007, **111**, 4596–4605.